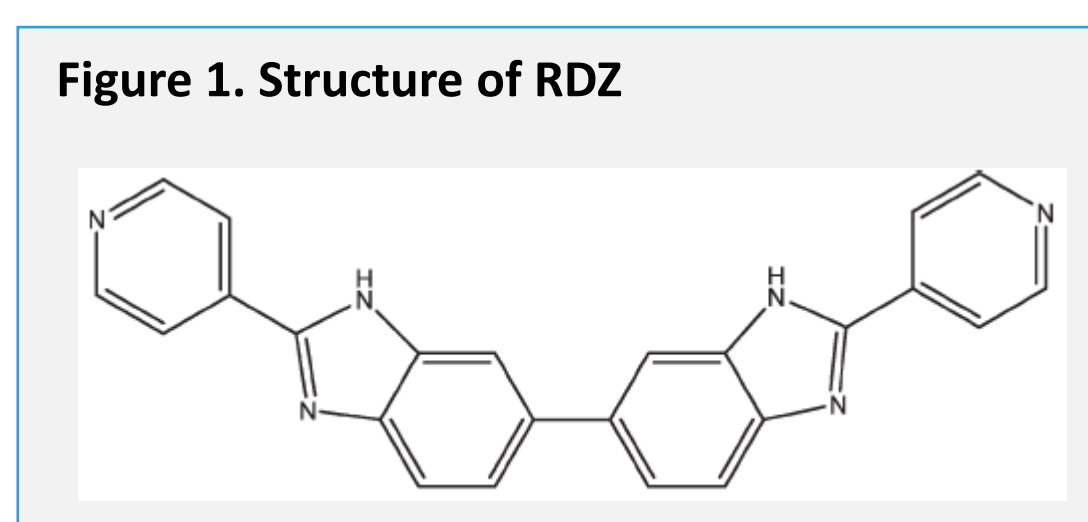


Transcriptomic analysis of the *Clostridioides difficile*-targeting antimicrobial ridinilazole implicates disruption of energy-generation pathways as its mechanism of action

Clive S Mason¹, Tim Avis¹, Nabeetha Nagalingam¹, Manikhandan Mudaliar¹, Chris Coward^{1*}, Esther Duperch¹, Keith R. Fox² and David J Powell¹¹Summit Therapeutics, Abingdon & Cambridge, UK; ²University of Southampton, UK; *Presenting author: chris.coward@summitplc.com

INTRODUCTION

- Clostridioides difficile* is among the top 5 pathogens identified as urgent public health threats by the US Centers for Disease Control and Prevention¹.
- Ridinilazole (RDZ) is an investigational bisbenzimidazole oral antimicrobial being developed by Summit Therapeutics which targets *C. difficile* whilst sparing the gut microbiome and its ability to produce protective secondary bile acids^{2,3}.
- Whilst currently in clinical development, the precise mechanism by which RDZ exerts its bactericidal activity has not been fully elucidated.
- RDZ is a symmetrical small-molecule drug with a head-to-head bisbenzimidazole core (Figure 1) and has intrinsic fluorescence properties that are enhanced by interaction with DNA⁴.
- We have previously shown that RDZ binding to polymeric dsDNA is specific for AT-rich molecules and tight binding was observed to dsDNA oligonucleotides with an AT-core. In these assays dissociation constants as low as 21 nM (10 ng/mL) were recorded⁵ which is much lower than the minimal inhibitory concentration for RDZ against *C. difficile* (0.125 µg/mL in BHI broth)⁶.



- We present DNase I footprinting studies to further characterize the DNA-binding specificity of RDZ and transcriptomics to elucidate the cellular response of *C. difficile* vegetative cells to RDZ exposure.

METHODS

DNase I footprinting

- Synthetic dsDNA molecules were cloned into pUC18 or pUC19 and used to prepare fragments that were labelled at the 3'-end with ³²P[dATP].
- AT5a and AT5b contained all 16 arrangements of (A/T)₅ with CGTG/CACG spacers cloned in opposite orientations.
- HexA and HexARev together contained 32 symmetrical hexanucleotide sequences cloned in opposite orientations
- DNase I footprinting was performed⁷ by mixing radiolabelled DNA with a titration of RDZ, incubating at 37°C for 1-30 min, digesting for 1 min with DNase I and the products separated on 8% denaturing polyacrylamide gels containing 8 M urea. Gels were fixed in 10% acetic acid, transferred to Whatmann 3MM paper, exposed to a storage phosphor screen overnight and scanned with a Typhoon phosphorimager.

RNAseq Transcriptomics

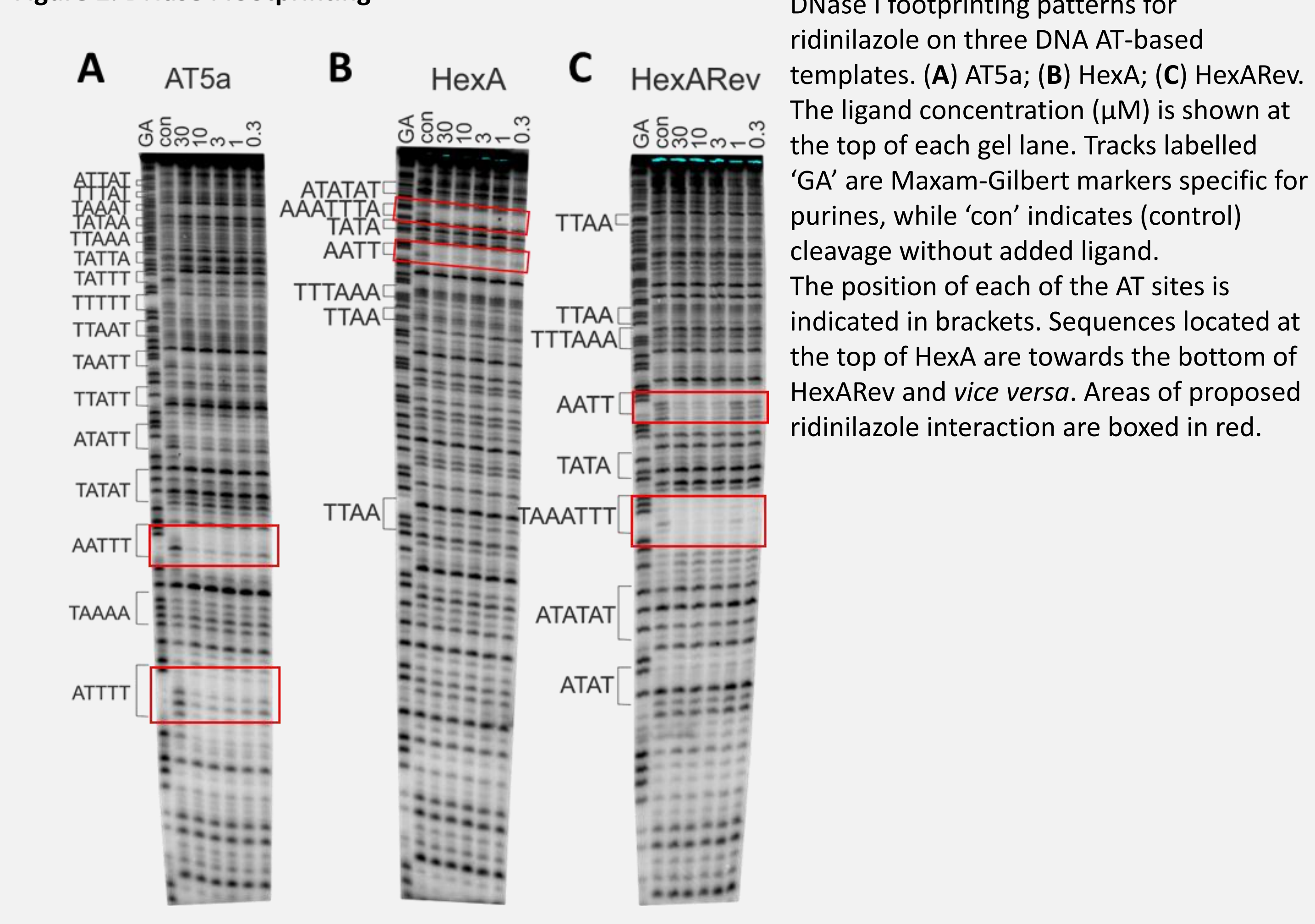
- C. difficile* 630 was grown overnight (16 h) in BHIS + 0.1% L-cysteine + 0.1% sodium taurocholate under anaerobic conditions and subcultured 1 in 100 into BHIS + 0.1% L-cysteine. At A600nm~0.4 (5-6 h growth) the culture was diluted 1 in 10 to initiate quadruplicate 40 mL assay cultures for each condition (RDZ at 4x MIC or DMSO control) and timepoint (15 min, 1 h, 2 h, 3 h)
- At each timepoint bacteria were harvested by centrifugation, resuspended in 1 mL RNAprotect (QIAGEN), pelleted, supernatant aspirated and stored at -80°C prior to RNA extraction using the RNeasy® Mini Kit (QIAGEN).
- Ribosomal RNA was removed with the Ribo-Zero™ rRNA Removal Kit (Illumina), cDNA made using TruSeq® Stranded mRNA Library Prep (Illumina), normalised and pooled prior to sequencing on a NextSeq 550 sequencer (Illumina) with single-ended 76 cycles.
- Data quality was examined using FastQC (v0.11.9) and FastQ Screen (v0.14.1). Quality and adapter trimming was performed using Trim Galore (v0.6.6; Cutadapt v3.4; Python v3.9.2). Reads were aligned to the *C. difficile* 630 genome (assembly name: ASM920v2) using Bowtie 2 (v2.4.2). Alignment quality was examined using Picard tools (v2.25.0) and samtools (v1.12.2-gd515e1b). Aligned reads were assigned to genes using Subread featureCounts (v2.0.2).
- The RNA-seq count table was imported into R (v4.0.4), normalized by trimmed mean of M values (TMM) and transformed to log2 count-per-million (CPM) using edgeR (v3.32.1). Principal Component Analysis (PCA) was performed using the top 500 variable genes or all genes in the genome and two outlier samples (RDZ_2h_4 and dms0_2h_4) were removed. Differential expression analysis was performed using DESeq2 (v1.30.1). Enrichment of KEGG pathways in differentially expressed genes were analysed using limma (v3.46.0) and KEGG pathway maps were generated using pathview (v1.30.1). Expression of 163 genes that are involved in oxidative phosphorylation, bacterial chemotaxis, cationic antimicrobial peptide resistance and Stickland metabolism pathways, and the top 100 differentially expressed genes (based on fold-change at 15 min; padj < 0.01) were visualized in a heatmap generated using pheatmap (v1.0.12).

RESULTS

DNase I footprinting

- Using the AT5a template the clearest footprint was obtained for AATTT (Figure 2), persisting to [RDZ] below 1 µM. AATTT was also a good binding site with ATATT, TAATT and TTTT showing weaker attenuated cleavage at the highest concentrations.
- For the HexA and HexARev substrates, clear footprints were observed at AAATTTA (HexA) and TAAATTT (HexB). AATT was also a good binding site.
- These data confirm a clear preference for RDZ binding to AT-rich sequences with good binding sites lacking a TpA step in the middle of the sequence

Figure 2. DNase I footprinting

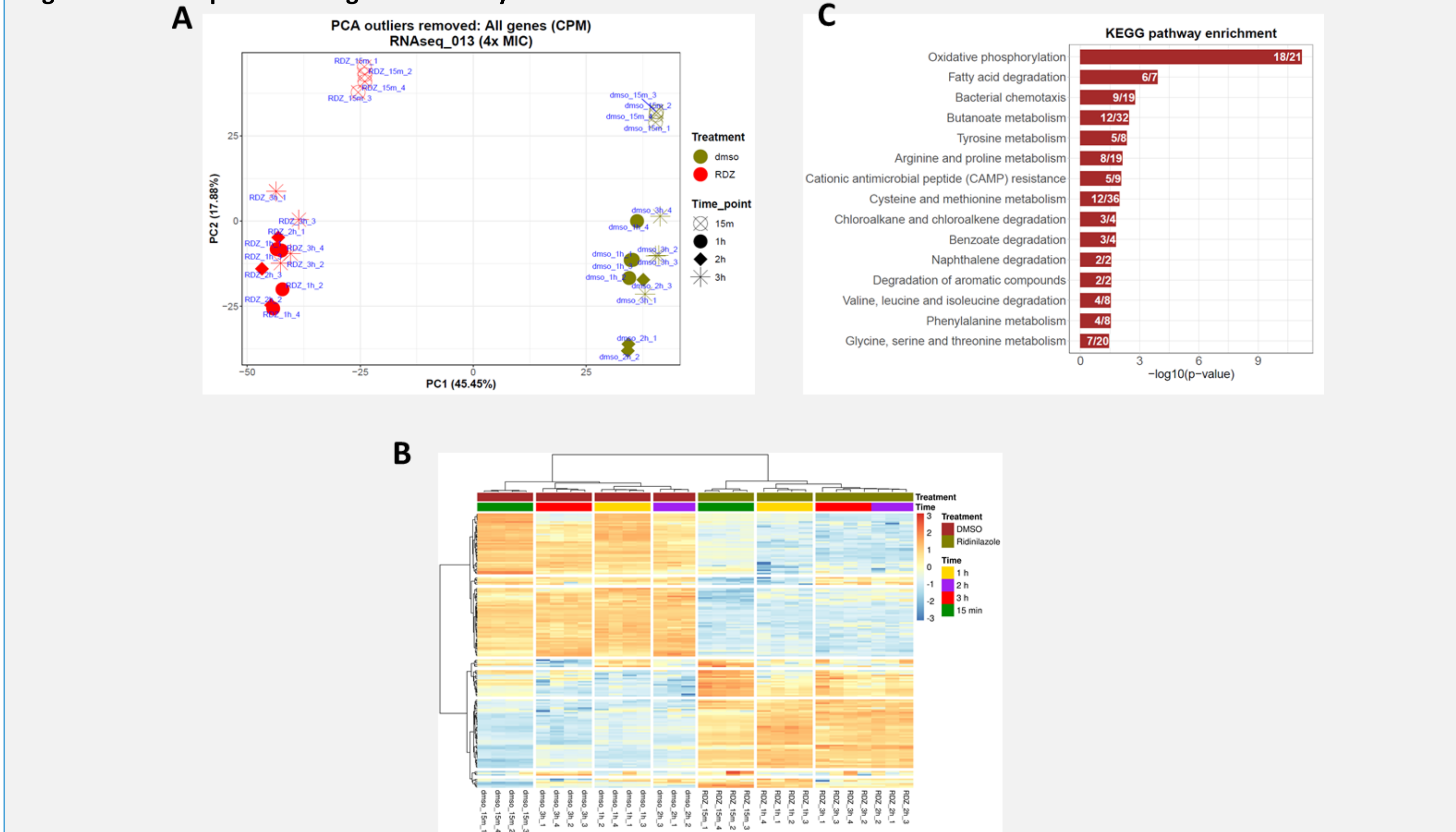


DNase I footprinting patterns for ridinilazole on three DNA AT-based templates. (A) AT5a; (B) HexA; (C) HexARev. The ligand concentration (µM) is shown at the top of each gel lane. Tracks labelled 'GA' are Maxam-Gilbert markers specific for purines, while 'con' indicates (control) cleavage without added ligand. The position of each of the AT sites is indicated in brackets. Sequences located at the top of HexA are towards the bottom of HexARev and vice versa. Areas of proposed ridinilazole interaction are boxed in red.

Transcriptomics – ridinilazole induces pleiotropic transcriptional dysregulation including alteration of energy metabolism pathways

- RNAseq elucidated the transcriptional consequences of exposure of *C. difficile* to RDZ at 4x MIC.
- PCA and heatmap analysis showed that transcriptional changes were established by 15 min post-exposure and persist for at least 3 h (Figure 3A & B).
- Further analysis focussed on the 15 min timepoint where upregulation of 325 and downregulation of 407 genes was observed indicating a rapid pleiotropic response.
- The entire glycine reductase (GR) operon (*grdX grdY grdZ grdA2 grdEABCD*) was in the top 60 most upregulated genes.
- Genes in the proline reductase (PR) operon (*prdABDE prdE2 prdF*) were among the most downregulated.
- GR and PR are key components of the Stickland pathway which couples oxidation and reduction of amino acid pairs to the formation of ATP and is the major mechanism by which *C. difficile* generates energy.
- We also observed expression changes in other genes in the Stickland pathway (Table 1).
- KEGG pathway analysis implicated 15 pathways in the response to RDZ exposure (Figure 3C), six of these being involved in amino acid metabolism, and all the genes encoding the ATP synthase were downregulated (Table 1). The ATP synthase generates ATP using proton motive force (PMF). PR is coupled to PMF generation by an uncharacterised mechanism⁸.
- These alterations in key ATP-generating pathways may affect the ability of *C. difficile* to produce energy, ultimately resulting in bacterial cell death.
- The cationic antimicrobial peptide (CAMP) resistance pathway *dltDABC* operon, encoding D-alanine transferase, was downregulated. This adds D-alanine to the cell wall reducing sensitivity to host CAMPs⁹. If this downregulation also occurs *in vivo*, RDZ exposure may increase the susceptibility *C. difficile* to host defense mechanisms.

Figure 3. Transcriptional changes induced by ridinilazole



(A) PCA scores from all genes in *C. difficile* strain 630 treated with 4x MIC ridinilazole or DMSO at 15 min, 1 h, 2 h and 3 h post-exposure. PC 1 & 2 together account for 63.33% of variance in the dataset (B) Heatmap of 163 genes (top 100 differentially expressed genes and the genes involved in oxidative phosphorylation, bacterial chemotaxis, cationic antimicrobial peptide (CAMP) resistance and Stickland metabolism pathways). The rows represent genes and the columns represent samples from all four time points; Red: increased expression in RDZ vs DMSO; Blue: reduced expression (C) KEGG pathway enrichment at 15 min time point. The bars represent the negative logarithm (base 10) of the enrichment P-values. The numbers inside the bars represent the ratio of the number of differentially expressed genes in the query set and the total number of genes in the pathway.

Table 1. Energy-metabolism genes differentially expressed on 15 min ridinilazole exposure

Gene Name	UniProt Protein Name	log ₂ FC	padj
Genes in the Stickland metabolic pathway			
<i>grdB</i>	Glycine reductase complex component B gamma subunit	9.18	2.23E-298
<i>grdA</i>	Glycine reductase complex selenoprotein A	8.94	0
<i>grdC</i>	Glycine reductase complex component C subunit beta	8.32	0
<i>grdD</i>	Glycine reductase complex component C subunit alpha	7.98	0
<i>grdX</i>	Putative glycine reductase complex component	6.63	0
<i>adhE1</i>	Aldehyde-alcohol dehydrogenase	3.65	6.91E-135
<i>adhE</i>	Aldehyde-alcohol dehydrogenase	3.16	2.10E-49
<i>scrK</i>	Fructokinase	0.55	3.76E-04
<i>eutE</i>	Ethanolamine acetaldehyde oxidoreductase	0.39	2.35E-01
<i>ldhA</i>	D-lactate dehydrogenase	-0.24	2.31E-01
<i>CD630_01160</i>	Putative ferredoxin/flavodoxin oxidoreductase, alpha subunit	-2.10	8.56E-25
<i>ptb</i>	Phosphate butyryltransferase	-3.06	9.18E-203
<i>prdB</i>	Proline reductase	-4.62	4.40E-121
<i>prdF</i>	Proline racemase	-4.64	2.36E-113
<i>prdA</i>	D-proline reductase proprotein prdA	-4.64	1.68E-181
<i>prdE</i>	Proline reductase PrdE	-4.91	2.56E-199
<i>prdD</i>	Proline reductase PrdD	-4.99	1.98E-121
<i>prdR</i>	Transcriptional regulator, sigma-54-dependent	-0.39	3.74E-03
Genes in the oxidative phosphorylation pathway			
<i>CD630_34050</i>	Putative iron-only hydrogenase, electron-transferring subunit HymA-like	1.43	1.93E-39
<i>CD630_34060</i>	Putative iron-only hydrogenase, electron-transferring subunit HymB-like	1.35	1.14E-13
<i>CD630_34070</i>	Putative iron-only hydrogenase, catalytic subunit HymC-like	1.21	1.55E-15
<i>CD630_29610</i>	Uncharacterized protein	-2.07	5.23E-17
<i>atpD</i>	ATP synthase subunit beta	-2.53	1.18E-49
<i>atpI</i>	V-type ATP synthase subunit I	-2.58	3.86E-67
<i>atpB</i>	V-type ATP synthase beta chain	-2.65	6.77E-26
<i>atpA</i>	V-type ATP synthase alpha chain	-2.77	1.95E-47
<i>atpD</i>	V-type ATP synthase subunit D	-2.85	6.21E-44
<i>atpK</i>	V-type ATP synthase subunit K	-2.92	4.60E-26
<i>atpC</i>	V-type ATP synthase subunit C	-3.10	1.61E-38
<i>atpF</i>	V-type ATP synthase subunit F	-3.14	3.15E-34
<i>atpE</i>	V-type ATP synthase subunit E	-3.27	5.60E-20
<i>atpC1</i>	ATP hydrolase epsilon chain	-3.43	7.44E-75
<i>ppaC</i>	Pyrophosphate phospho-hydrolase	-3.82	6.84E-134
<i>atpG</i>	ATP synthase gamma chain	-3.86	1.26E-222
<i>atpA</i>	ATP synthase subunit alpha	-3.94	8.74E-232
<i>atpE</i>	ATP synthase subunit c	-4.04	1.53E-71
<i>atpH</i>	ATP synthase subunit delta	-4.34	2.34E-240
<i>atpF</i>	ATP synthase subunit b	-4.44	5.65E-124
<i>atpA2 atpB</i>	ATP synthase subunit a	-4.51	9.84E-223

CONCLUSIONS

- The small-molecule *C. difficile*-targeting antimicrobial ridinilazole which binds AT-rich DNA⁵ has particular affinity for AATT, AATTT, AAATTTA and TAAATTT sites.
- Exposure of *C. difficile* to ridinilazole *in vitro* results in rapid, long-lasting and pleiotropic alterations in gene expression.
- Energy metabolism, specifically key enzymes in the Stickland fermentation pathway and the ATP synthase, is dysregulated on ridinilazole exposure.

REFERENCES

¹CDC (2019) doi:10.15620/cdc.82532.; ²Thorpe, C. M. et al. (2018) *PLoS One* doi:10.1371/journal.pone.0199810; ³Qian, X. et al. (2020) *Am J Physiol Gastrointest Liver Physiol* doi:10.1152/ajpgi.00046.2020; ⁴Chaudhuri, P. et al. (2007) *J Org Chem* doi:10.1021/jo0619433; ⁵Mason, C. et al. (2021) *Open Forum Infect Dis* doi:10.1093/ofid/ofab466.1246; ⁶Corbett, D. et al. (2015) *J Antimicrob Chemother* doi:10.1093/jac/dkv006; ⁷Hampshire, A. J. et al. (2007) *Methods* doi:10.1016/j.jm.2007.01.002; ⁸Jackson, S. et al. (2006) *J Bact* doi:10.1128/JB.01370-06; ⁹McBride et al. (2011) *Microbiology* doi:10.1099/mic.0.045997-0